



Short Communication

Interface dipole induced threshold voltage shift in the $\text{Al}_2\text{O}_3/\text{GaN}$ heterostructureChuanju Wang, Xiaohang Li^{*}

Advanced Semiconductor Laboratory, Electrical and Computer Engineering Programs, CEMSE Division, King Abdullah University of Science and Technology (KAUST), Thuwal 23955, Saudi Arabia

A B S T R A C T

The $\text{Al}_2\text{O}_3/\text{GaN}$ heterostructure is a crucial component of GaN-based electronic and photonic devices, and the $\text{Al}_2\text{O}_3/\text{GaN}$ interface quality plays an important role in determining the device performance. Here, using density functional theory, we confirmed that dipole formed at the $\text{Al}_2\text{O}_3/\text{GaN}$ interface can be attributed to electron transfer and redistribution between Al_2O_3 and GaN. The formation of dipole was confirmed by X-ray photoemission spectroscopy. The dipole induced electric field at the interfaces of the $\text{Al}_2\text{O}_3/\text{GaN}$ heterostructures result in negative threshold voltage (V_{TH}) shifts of 2.3 and 1.2 V for the heterostructures without defects and with one Al interstitial (Al_i) defect, respectively. On the other hand, the Al_i defect can induce positive charges, resulting in negative V_{TH} shifts. Therefore, an improvement in the interface quality (i.e., by eliminating the Al_i defect) does not necessarily result in positive V_{TH} shifts. This study reveals novel electronic properties of the $\text{Al}_2\text{O}_3/\text{GaN}$ heterostructure and offers a path toward the achievement of GaN-based devices with engineered features.

1. Introduction

GaN-based, high electron mobility transistors (HEMTs) can deliver a high current, a high voltage, and high switching speeds. As such, they are widely used in high power and high radio frequency devices [1–3]. Gate dielectrics are widely used to suppress the gate leakage current and enlarge the gate breakdown voltage in GaN HEMTs [4,5]. The Al_2O_3 fabricated by atomic layer deposition (ALD) has been broadly adopted as a gate dielectric material owing to its superior electronic properties, including its high bandgap and dielectric constant [6–8]. However, although the Al_2O_3 obtained via ALD exhibits superior properties, numerous interface positive fixed charges and traps are introduced at the $\text{Al}_2\text{O}_3/\text{GaN}$ interface or in the bulk Al_2O_3 [8,9]. These positive, fixed charges can induce a negative threshold voltage (V_{TH}) shifts, hindering the development of enhancement-mode GaN HEMTs. Moreover, traps at the $\text{Al}_2\text{O}_3/\text{GaN}$ interface can result in reliability and stability challenges. [7,9–11] The occurrence of positive charges and traps at the $\text{Al}_2\text{O}_3/\text{GaN}$ interface can be attributed to the defects at the interface. Non-stoichiometric atomic ratios of O and Al have been found at the $\text{Al}_2\text{O}_3/\text{GaN}$ interface, with Al significantly surpassing O [12,13]. The Al-rich conditions can produce excess Al interstitial (Al_i) defects. Generally, structural impurities, such as Al_i defects and O vacancies, can introduce various defect levels in the Al_2O_3 bandgap [14,15]. The charged defect levels can behave like fixed charges or fast and slow traps depending on their energy levels in the bandgap [14,15]. When the energy states are

above the GaN conduction band edges, under either positive or negative gate stress on the $\text{Al}_2\text{O}_3/\text{GaN}$ heterostructure, the Fermi level can hardly modulate these energy levels. Thus, the defects behave similarly to fixed charges [10,14,15]. However, when the energy states are within the bandgap of GaN and close to the midgap, charge trapping and detrapping occurs when the Fermi level moves across the energy levels. Resultantly, the defects behave similarly to trap states [14,15]. Considerable efforts have been devoted to improving the interface quality between gate dielectrics and GaN [7,9,11]. Although the interface trap density can be reduced to an extremely low value, in many cases, the V_{TH} does not shift to a positive value accordingly or it may even shift to a more negative value [9,16]. As both the fixed charges and interface traps are ascribed to the interface defects [14,15], the positive charges thus the positive charges induced negative V_{TH} shifts should also be suppressed together with the interface trap density. The abnormal V_{TH} shifts after the improvement in the interface quality indicates that there are additional factors that contribute to the V_{TH} , which were not considered prior.

In addition to the interface charges and traps, interface dipoles control the interface electronic structures [17–23]. Generally, dipoles are formed between dielectrics and semiconductors or between two dielectrics, and they have a significant impact on the device performance. For example, dipoles formed at the HfO_2/Si interface have been found to negatively shift V_{TH} [17–19]. The origins of the dipoles are unclear; however, the formation of the Si–O–Hf bonds could be one

^{*} Corresponding author.E-mail address: xiaohang.li@kaust.edu.sa (X. Li).<https://doi.org/10.1016/j.apsusc.2023.156954>

Received 2 January 2023; Received in revised form 18 February 2023; Accepted 3 March 2023

Available online 9 March 2023

0169-4332/© 2023 The Author(s). Published by Elsevier B.V. This is an open access article under the CC BY license (<http://creativecommons.org/licenses/by/4.0/>).

reason for the dipole formation [17,19]. Dipoles were also widely found at high-k/SiO₂ interface, and the magnitude of the V_{TH} shifts relies on the employed high-k materials [20–22]. The electronegativity difference between the cations of high-k and SiO₂ is regarded as one reason for the dipole formation [22]. Another possible reason is the oxygen density difference at the junctions between the high-k materials and SiO₂ [20]. Moreover, dipole formation could occur between two high-k materials, such as HfO₂ and Al₂O₃, and dipoles at the HfO₂/Al₂O₃ interface have been applied to explain the abrupt V_{TH} shifts [23]. Based on these results, we hypothesize that dipoles can be formed at the Al₂O₃/GaN interface. In addition to the defect induced charges, dipoles could be an additional factor affecting the V_{TH} of the Al₂O₃/GaN heterostructure.

2. Experiments

We perform spin-polarized first principles calculations within the framework DFT, as implemented in the Vienna ab-initio simulation package. The total energy convergence threshold is set to 10⁻⁶ eV and the structures are optimized until the Hellmann-Feynman forces stay below 0.01 eV/Å. All the calculations are performed within the Perdew-Burke-Ernzerhof generalized gradient approximation. An energy cutoff of 450 eV is used in the plane wave expansion. The θ -phase Al₂O₃ was adopted to build the Al₂O₃/GaN heterostructure, as its bandgap and mass density values are similar to those of amorphous Al₂O₃ grown by ALD [8]. The bottom dangling bonds of GaN in the Al₂O₃/GaN heterostructures were passivated by pseudohydrogen with 0.75 valence electrons to ensure that the density of states in the bandgap are from the interface defects [24]. In the subsequent DFT calculations, one Al_i defect was introduced into the Al₂O₃/GaN interface to evaluate its effect on the electronic properties. For the X-ray photoemission spectroscopy (XPS) measurements, 1.2 nm Al₂O₃ was deposited on the surface GaN (0001). Before the ALD Al₂O₃ film growing process, the GaN substrates were cleaned with diluted hydrochloric acid for 3 min to remove the surface native oxide layers. Subsequently, the GaN substrates were transferred to the ALD chamber for Al₂O₃ deposition. One ALD Al₂O₃ cycle comprised a 0.015 s trimethyl aluminum dose pulse and a 4 s O₂ plasma oxidation, followed by a 3 s purge with N₂. The ALD Al₂O₃ growth per cycle was 1.2 Å, measured by an ellipsometer.

3. Results and discussion

The insets of Fig. 1(a) and (b) show the atomic structures of the Al₂O₃/GaN interface regions without and with one Al_i defect, respectively. The Al_i defect is indicated by an arrow in Fig. 1(b). After introducing one Al_i defect, the atomic positions of Al, Ga, and O were severely distorted at the interface compared with the case of the heterostructure without defects. For the Al₂O₃/GaN heterostructure without the Al_i defect, eight Ga–O bonds were initially observed at the interface, with

the eight oxygen atoms perfectly saturating the eight Ga dangling bonds [8]. The N–Ga–O–Al interface bonding used in this study is the most stable interface configuration of the Al₂O₃/GaN heterostructure [25]. Fig. 1(a) shows the total density of states (TDOS) without the Al_i defect. The electron counting rule was satisfied in the Al₂O₃/GaN heterostructure, thus leading to an insulating interface with a clean bandgap. The strong peak located at 3.2 eV can be attributed to contribution from the Al atoms (Fig. S1 and 2). However, as shown in Fig. 1(b), gap states occur after the introduction of the Al_i defect. In addition, the Al₂O₃/GaN heterostructure with the Al_i defect has a large TDOS close to 3.2 eV, therefore, the peak located at 3.2 eV of the heterostructure without the Al_i defect is not observable. As discussed above, the interface states occur in the bandgap can behave as traps or fixed charges, thereby deteriorating the device performance.

Charge density difference was calculated to analyze the role of Al_i defects on the charge transfer and redistribution at the Al₂O₃/GaN interfaces. The electron densities of Al₂O₃ and GaN were subtracted from those of the Al₂O₃/GaN heterostructures. Fig. 2(a) and (b) show the Al₂O₃/GaN heterostructures without and with the Al_i defect, respectively. The charge transfer and redistribution primarily occur at the N–Ga–O–Al layer, with negligible change on charge density in the inner Al₂O₃ and GaN far away from the interfaces. The charge density difference at the Al₂O₃/GaN interfaces indicates electron transfer from GaN to Al₂O₃ across the interfaces. Charge accumulation (yellow part) primarily occurs around the O layer in Al₂O₃, with a small accumulation area observed around the N layer in GaN; furthermore, strong charge depletion (light blue part) occurs around the Ga layer in GaN, with a small depletion area observed around the Al layer in Al₂O₃. Consequently, in the equilibrium state, dipoles form at the Al₂O₃/GaN interfaces without and with the Al_i defect as the built-in electric field is established. The built-in electric field is oriented from GaN to the Al₂O₃, which can induce a negative V_{TH} shifts. As shown in Fig. 2(b), after interposing one Al_i defect, the charge accumulation around the O layer and charge depletion around the Ga layer reduced considerably. Consequently, the dipole induced electric field could be effectively attenuated accordingly. The dipole induced V_{TH} shifts in the Al₂O₃/GaN heterostructures without and with the Al_i defect can be estimated based on the equation [23]:

$$V_{TH} = - \left(\frac{\int_0^{d_1} dz \int Q(x, y, z) dx dy + \int_0^{d_2} dz \int Q(x, y, z) dx dy}{\epsilon_{GaN}} + \frac{\int_0^{d_3} dz \int Q(x, y, z) dx dy + \int_0^{d_4} dz \int Q(x, y, z) dx dy}{\epsilon_{Al_2O_3}} \right)$$

where d_1 , d_2 and d_3 , d_4 shown in Fig. 2(a) and (b) are the widths of the dipole layer across the GaN and Al₂O₃ layers, respectively. As shown in Fig. 2(a), the values of d_1 , d_2 , d_3 , and d_4 are 1.72, 1.62, 1.14, and 1.72 Å,

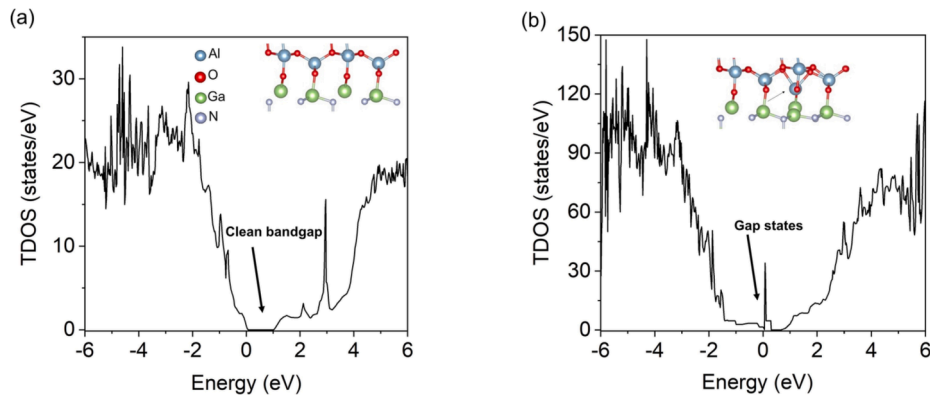


Fig. 1. (a) Total density of states of the Al₂O₃/GaN heterostructures (a) without and (b) with the Al_i defect. Inset shows the atomic structure configuration at the interfaces where the Al_i defect is indicated by an arrow in (b).

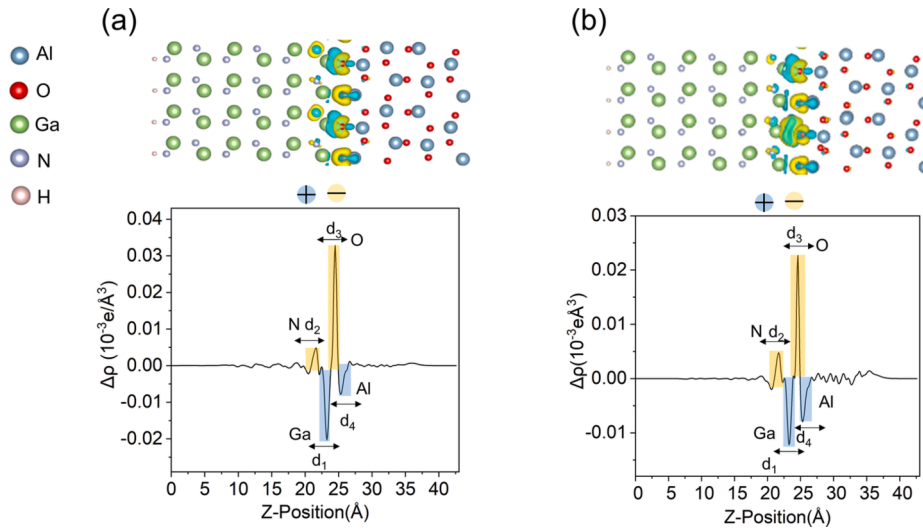


Fig. 2. Charge density differences of $\text{Al}_2\text{O}_3/\text{GaN}$ heterostructures (a) without and (b) with the Al_I defect and the corresponding planar-averaged, electron density difference of the heterostructures.

respectively. As shown in Fig. 2 (b), the values of d_1 , d_2 , d_3 , and d_4 are 1.72, 1.52, 0.95, and 1.62 Å, respectively. $Q(r)$ is the volume charge density; ϵ_{GaN} and $\epsilon_{\text{Al}_2\text{O}_3}$ are the dielectric constants of GaN and Al_2O_3 , respectively. According to the equation, the negative V_{TH} shifts of 2.3 V can be reduced to 1.2 V after interposing one Al_I defect. The DFT results here imply that even without any interface defects, owing to the electron transfer and redistribution at the $\text{Al}_2\text{O}_3/\text{GaN}$ interfaces, the dipole induced electric field can still induce a negative V_{TH} shifts. Therefore, the dipole formed at the interface is the intrinsic property of the $\text{Al}_2\text{O}_3/\text{GaN}$ heterostructure, and thus, it cannot be eliminated by removing the interface defects. In addition, the above DFT calculation was based on the Ga-polar GaN. However, for the N-polar GaN, charge transfer will also across the N-Ga-N-Al interface chemical bonds where the interface dipole forms at the interface of the $\text{Al}_2\text{O}_3/\text{GaN}$ (N-polar) heterostructure.

The Al_I defect in Al_2O_3 can introduce positive charges and induce a negative V_{TH} shifts [14,15,26]. Therefore, after eliminating the Al_I defect, the defect induced negative V_{TH} shifts will be suppressed. Substantial efforts have been devoted to improving the interface quality between Al_2O_3 and GaN [7,9,11]. Although the interface trap density can be reduced to an extremely small value, the V_{TH} does not change correspondingly or it may even exhibit a negative shift [9,16]. As both the fixed charges and interface traps are ascribed to the defects at the interface [14,15], the positive charges and the positive charges induced negative V_{TH} shifts should be suppressed together with the interface trap density. In this study, the abnormal V_{TH} movement after interface

quality improving of the $\text{Al}_2\text{O}_3/\text{GaN}$ heterostructures is attributed to the dipole induced negative V_{TH} shifts can be increased from 1.2 to 2.3 V after removing the Al_I defect at the interface. Except from positive charge induced negative V_{TH} shifts, dipole is an additional factor that can modulate the V_{TH} in the $\text{Al}_2\text{O}_3/\text{GaN}$ heterostructure. Fig. 3(a) shows the Ga 3d XPS spectra of the $\text{Al}_2\text{O}_3/\text{GaN}$ heterostructure and pristine GaN. The XPS peak located at 19.7 eV corresponds to Ga-N bond in the pristine GaN, while the Ga-O bond located at 20.7–20.9 eV is absent in the $\text{Al}_2\text{O}_3/\text{GaN}$ heterostructure [27]. Therefore, no oxidation occurs during the ALD process. Compared with that for the pristine GaN, after the heterostructure formation, the binding energy of Ga 3d shifts toward a lower value (~ 0.5 eV). Additionally, N 1s XPS spectra also shifts to a smaller value after Al_2O_3 coating (Fig. S3). Based on the above DFT calculation results, it was established that electron redistribution mainly occurred at the $\text{Al}_2\text{O}_3/\text{GaN}$ interface, and the dipole induced electric field is oriented from GaN to Al_2O_3 . Fig. 3(b) shows the band alignment diagram of the $\text{Al}_2\text{O}_3/\text{GaN}$ heterostructure before and after Al_2O_3 coating. Owing to the dipole induced electric field, upward band bending occurs at the interface of the $\text{Al}_2\text{O}_3/\text{GaN}$ heterostructure (0.48 eV), which can shift the binding energy of Ga 3d toward a lower value [28]. The value of band bending was obtained from the valence band spectra (Fig. S4). Fig. 4(a) and (b) display 2D electron localization function (ELF) profiles of $\text{Al}_2\text{O}_3/\text{GaN}$ heterostructures without and with the Al_I defect, respectively. The ELF value varies from 0 to 1, where the value smaller than 0.5 indicates the delocalization of the electrons and a larger value indicates the stronger ability to accumulate electrons [29].

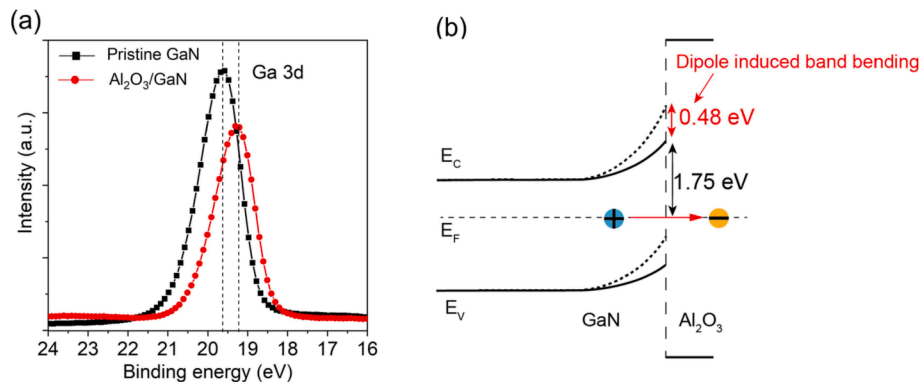


Fig. 3. (a) Ga 3d XPS spectra for the $\text{Al}_2\text{O}_3/\text{GaN}$ heterostructure and pristine GaN. (b) Schematic band alignment diagram of the $\text{Al}_2\text{O}_3/\text{GaN}$ heterostructure where the dipole induced electric field is also shown. The solid and dashed lines correspond to the band bending before and after Al_2O_3 coating.

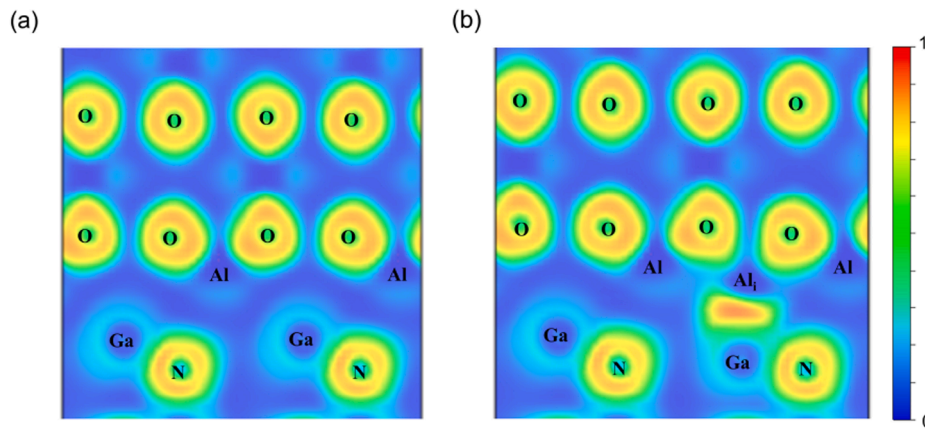


Fig. 4. 2D ELF profiles of $\text{Al}_2\text{O}_3/\text{GaN}$ heterostructures (a) without and (b) with the Al_I defect.

The charge depletion and accumulation of each atom are labeled correspondingly in Fig. 4(a) and (b). After interposing one Al_I defect, strong electron accumulation occurs between the Ga atoms and Al_I defects, indicating the formation of Ga–Al bonds at the $\text{Al}_2\text{O}_3/\text{GaN}$ interface. The strong electron accumulation accounts for the stability of the $\text{Al}_2\text{O}_3/\text{GaN}$ heterostructure with the Al_I defect. The Ga–Al bond can potentially change the polarity of the GaN surface from the Ga face to the N face [10,30]. As Ga-face and N-face GaN exhibit polarization charge densities of -2×10^{13} and $2 \times 10^{13} \text{ cm}^{-2}$, respectively [31], the inversion of the polarity charge could be one source of the positive charges at the $\text{Al}_2\text{O}_3/\text{GaN}$ interface.

4. Conclusions

In summary, we confirmed that dipoles formed at the $\text{Al}_2\text{O}_3/\text{GaN}$ interface can be attributed to the electron transfer between Al_2O_3 and GaN. The magnitude of the dipole induced V_TH shifts can be reduced after improving the interface quality (eliminating the Al_I defect). Moreover, we found that the Al_I defect forms a stable bond with the Ga atom (Al–Ga), indicating the stability of the $\text{Al}_2\text{O}_3/\text{GaN}$ heterostructure with the Al_I defect. In addition, because charge transfer and redistribution are fundamental properties of the interface chemistry of two dissimilar interfaces, we propose that dipole formation could occur at other high-k material/semiconductor interfaces, such as $\text{Ga}_2\text{O}_3/\text{GaN}$, SiN/GaN , and $\text{Al}_2\text{O}_3/\text{Si}$ heterostructures.

CRediT authorship contribution statement

Chuanju Wang: Conceptualization, Methodology, Validation, Investigation, Writing – original draft, Writing – review & editing.
Xiaohang Li: Resources, Project administration, Funding acquisition.

Declaration of Competing Interest

The authors declare the following financial interests/personal relationships which may be considered as potential competing interests: Chuanju wang reports was provided by KAUST. Chuanju wang reports a relationship with King Abdullah University of Science and Technology that includes: employment.

Data availability

No data was used for the research described in the article.

Appendix A. Supplementary data

Supplementary data to this article can be found online at <https://doi.org/10.1016/j.apsusc.2023.156954>.

References

- [1] U.K. Mishra, P. Parikh, Y.-F. Wu, AlGaIn/GaN HEMTs—an overview of device operation and applications, *Proc. IEEE*, 90 (6) (2002) 1022–1031.
- [2] Y.-F. Wu, D. Kapolnek, J.P. Ibbetson, P. Parikh, B.P. Keller, U.K. Mishra, Very-high power density AlGaIn/GaN HEMTs, *IEEE Trans. Electron Devices* 48 (3) (2001) 586–590.
- [3] Y.-F. Wu, A. Saxler, M. Moore, R. Smith, S. Sheppard, P. Chavarkar, T. Wisleder, U. Mishra, P. Parikh, 30-W/mm GaN HEMTs by field plate optimization, *IEEE Electron Device Lett.* 25 (3) (2004) 117–119.
- [4] C. Liu, E.F. Chor, L.S. Tan, Enhanced device performance of AlGaIn/GaN HEMTs using HfO_2 high-k dielectric for surface passivation and gate oxide, *Semicond. Sci. Technol.* 22 (5) (2007) 522.
- [5] Y. Hao, L. Yang, X. Ma, J. Ma, M. Cao, C. Pan, C. Wang, J. Zhang, High-performance microwave gate-recessed AlGaIn/AlN/GaN MOS-HEMT with 73% power-added efficiency, *IEEE Electron Device Lett.* 32 (5) (2011) 626–628.
- [6] X. Liu, C. Jackson, F. Wu, B. Mazumder, R. Yeluri, J. Kim, S. Keller, A. Arehart, S. Ringel, J. Speck, Electrical and structural characterizations of crystallized $\text{Al}_2\text{O}_3/\text{GaN}$ interfaces formed by in situ metalorganic chemical vapor deposition, *J. Appl. Phys.* 119 (1) (2016) 015303.
- [7] Y. Ando, K. Nagamatsu, M. Deki, N. Taoka, A. Tanaka, S. Nitta, Y. Honda, T. Nakamura, H. Amano, Low interface state densities at $\text{Al}_2\text{O}_3/\text{GaN}$ interfaces formed on vicinal polar and non-polar surfaces, *Appl. Phys. Lett.* 117 (10) (2020) 102102.
- [8] Z. Zhang, Y. Guo, J. Robertson, Chemical bonding and band alignment at $\text{X}_2\text{O}_3/\text{GaN}$ ($\text{X} = \text{Al}, \text{Sc}$) interfaces, *Appl. Phys. Lett.* 114 (16) (2019) 161601.
- [9] S. Yang, Z. Tang, K.-Y. Wong, Y.-S. Lin, C. Liu, Y. Lu, S. Huang, K.J. Chen, High-Quality Interface in $\text{Al}_2\text{O}_3/\text{GaN}/\text{AlGaIn}/\text{GaN}$ MIS Structures With In Situ Pre-Gate Plasma Nitridation, *IEEE Electron Device Lett.* 34 (12) (2013) 1497–1499.
- [10] M. Esposito, S. Krishnamoorthy, D.N. Nath, S. Bajaj, T.-H. Hung, S. Rajan, Electrical properties of atomic layer deposited aluminum oxide on gallium nitride, *Appl. Phys. Lett.* 99 (13) (2011) 133503.
- [11] Y. Cai, W. Liu, M. Cui, R. Sun, Y.C. Liang, H. Wen, L. Yang, S.N. Supardan, I.Z. Mitrovic, S. Taylor, Effect of surface treatment on electrical properties of GaN metal–insulator–semiconductor devices with Al_2O_3 gate dielectric, *Jpn. J. Appl. Phys.* 59 (4) (2020) 041001.
- [12] C. Wang, F. AlQatari, V. Khandelwal, R. Lin, X. Li, Origin of interfacial charges of $\text{Al}_2\text{O}_3/\text{Si}$ and $\text{Al}_2\text{O}_3/\text{GaN}$ heterogeneous heterostructures, *Appl. Surf. Sci.* 608 (2022) 155099.
- [13] C. Wang, X. Li, Correlative atomic coordination and interfacial charge polarity in $\text{Al}_2\text{O}_3/\text{GaN}$ and $\text{Al}_2\text{O}_3/\text{Si}$ heterostructures, *Phys. Status Solidi-Rapid Res. Lett.* 202200413 (2022).
- [14] J. Weber, A. Janotti, C. Van de Walle, Native defects in Al_2O_3 and their impact on III–V/ Al_2O_3 metal-oxide-semiconductor-based devices, *J. Appl. Phys.* 109 (3) (2011) 033715.
- [15] M. Choi, A. Janotti, C.G. Van de Walle, Native point defects and dangling bonds in $\alpha\text{-Al}_2\text{O}_3$, *J. Appl. Phys.* 113 (4) (2013) 044501.
- [16] F. Guo, S. Huang, X. Wang, T. Luan, W. Shi, K. Deng, J. Fan, H. Yin, J. Shi, F. Mu, Suppression of interface states between nitride-based gate dielectrics and ultrathin-barrier AlGaIn/GaN heterostructure with in situ remote plasma pretreatments, *Appl. Phys. Lett.* 118 (9) (2021) 093503.
- [17] N. Miyata, Y. Abe, T. Yasuda, Conductance spectroscopy study on interface electronic states of HfO_2/Si structures: Comparison with interface dipole, *Appl. Phys. Express.* 2 (3) (2009) 035502.
- [18] N. Miyata, T. Yasuda, Y. Abe, Kelvin probe study of dipole formation and annihilation at the HfO_2/Si interface, *Appl. Phys. Express.* 3 (5) (2010) 054101.
- [19] N. Miyata, T. Yasuda, Y. Abe, Kelvin probe study on formation of electric dipole at direct-contact HfO_2/Si interfaces, *J. Appl. Phys.* 110 (7) (2011) 074115.
- [20] K. Kita, A. Toriumi, Origin of electric dipoles formed at high-k/ SiO_2 interface, *Appl. Phys. Lett.* 94 (13) (2009) 132902.
- [21] L. Lin, J. Robertson, Atomic mechanism of electric dipole formed at high-k: SiO_2 interface, *J. Appl. Phys.* 109 (9) (2011) 094502.

- [22] P.D. Kirsch, P. Sivasubramani, J. Huang, C. Young, M. Quevedo-Lopez, H. Wen, H. Alshareef, K. Choi, C. Park, K. Freeman, Dipole model explaining high-k/metal gate field effect transistor threshold voltage tuning, *Appl. Phys. Lett.* 92 (9) (2008) 092901.
- [23] J. Son, V. Chobpattana, B.M. McSkimming, S. Stemmer, Fixed charge in high-k/GaN metal-oxide-semiconductor capacitor structures, *Appl. Phys. Lett.* 101 (10) (2012) 102905.
- [24] J. Li, L.-W. Wang, Band-structure-corrected local density approximation study of semiconductor quantum dots and wires, *Phys. Rev. B* 72 (12) (2005) 125325.
- [25] K. Chokawa, E. Kojima, M. Araidai, K. Shiraishi, Investigation of the GaN/Al₂O₃ interface by first principles calculations, *Phys. Status Solidi B* 255 (4) (2018) 1700323.
- [26] A. Calzolaro, T. Mikolajick, A. Wachowiak, Status of Aluminum Oxide Gate Dielectric Technology for Insulated-Gate GaN-Based Devices, *Mater.* 15 (3) (2022) 791.
- [27] H. Henck, Z.B. Aziza, O. Zill, D. Pierucci, C.H. Naylor, M.G. Silly, N. Gogneau, F. Oehler, S. Collin, J. Brault, Interface dipole and band bending in the hybrid p–n heterojunction MoS₂/GaN (0001), *Phys. Rev. B* 96 (11) (2017) 115312.
- [28] K. Kim, M. Hua, D. Liu, J. Kim, K.J. Chen, Z. Ma, Efficiency enhancement of InGaN/GaN blue light-emitting diodes with top surface deposition of AlN/Al₂O₃, *Nano Energy* 43 (2018) 259–269.
- [29] X. Guo, Z. Lu, Y.-G. Jung, J. Zhang, *Novel Lanthanum Zirconate-based Thermal Barrier Coatings for Energy Applications*, Springer, 2020.
- [30] M.H. Wong, F. Wu, J.S. Speck, U.K. Mishra, Polarity inversion of N-face GaN using an aluminum oxide interlayer, *J. Appl. Phys.* 108 (12) (2010) 123710.
- [31] B.J. Rodriguez, A. Gruverman, A. Kingon, R. Nemanich, O. Ambacher, Piezoresponse force microscopy for polarity imaging of GaN, *Appl. Phys. Lett.* 80 (22) (2002) 4166–4168.